Vertical Circulation Revealed by Diurnal Heating of the Upper Ocean in Late Winter. Part II: Modeling

KAREN J. H. THOMAS

Institute of Oceanographic Sciences, Wormley, Godalming, Surrey, UK

(Manuscript received 8 March 1988, in final form 27 June 1988)

ABSTRACT

A heat budget for observations at current meters in the mixing layer beneath a freely drifting spar buoy showed that the buoy must be in a convergence zone, where transport of warm water downwards enhances the diurnal heating effect. The convergence zone is probably associated with Langmuir circulations due to the strong, steady wind experienced before and during the 6-day deployment.

This paper describes a two-dimensional numerical model of a Langmuir cell imposed on a mixed layer. The processes of advection and mixing occur separately at each time step, after surface heat fluxes have been absorbed. Since momentum is not allowed to mix, we consider the evolution of the temperature field when a diurnal heating cycle is imposed, and determine the influence of the imposed circulation on the heat budget of the mixing layer. To obtain the amplitude and phase observed in the diurnal heating signal, a vertical velocity of 1 cm s^{-1} is required in the model.

1. Introduction

Pollard and Thomas (1989, hereafter known as Part I) described a 6-day case study of diurnal heating and cooling in the mixing layer at a freely drifting spar buoy in the eastern North Atlantic during late winter 1984 (Fig. 1). Using five time series of temperatures at current meters (VACMs) suspended beneath the drifting buoy (Fig. 1b), the minimum heat flux required to heat the water column (from the surface to 150 m) to the observed temperatures was calculated for the 6-day deployment. This was compared with the net heat flux calculated from carefully calibrated meteorological observations. During the heating period of each day, the observed rise in temperature was found to be too large to be accounted for by the heat flux, and it also appeared that the column of water beneath the spar was cooling more at night than would be expected from the meteorological forcing. Using a combination of the observed currents and a SeaSoar survey of the surrounding waters during the deployment, the magnitude of the heating effect of horizontal advection was calculated. It was proved to be both too small and out of phase with the observed heating, and was discounted as a possible mechanism for the imbalance in the heat budget. The conclusion was reached that the spar buoy must have drifted into the convergence zone of one or more Langmuir circulations. This would enhance the diurnal heating signal by drawing in warmer water at the surface and carrying it downwards past the VACMs. This paper describes attempts to model the diurnal cycle of temperature measured at the current meters below the spar buoy.

Figure 2a shows part of the time series of temperatures observed at the VACMs at depths between 15 and 145 m in a mixing layer of about 200–250 m, as discussed in Part I. The data have been low-pass filtered to reduce internal wave noise. Only one day is plotted (7 March 1984, day 67), on which there was a large diurnal heating signal, 40 mK at 15 m, and 20 mK even at 145 m depth. Although this was the sunniest day, there is insufficient solar radiation to heat the water column by the observed amount; the heat available is 5.8 (±2.6) MJ m^{-2} while the heat required is 13.0 (±1.5) MJ m^{-2}. In addition, the diurnal heating is observed down to 145 m, beyond the depth to which solar radiation may penetrate; this suggests some vertical advection.

Since the heat budget of the layer does not balance, a one-dimensional model cannot be expected to reproduce the observed diurnal signal. Therefore a simple, quasi-two-dimensional model has been developed in order to study the effect of a Langmuir circulation cell on the mixing and heating of the mixed layer. It was hoped that this would simulate the temperature time series at the VACMs beneath the drifting spar buoy. In this way the magnitude of the vertical velocity required at the VACMs might be estimated. Before

Corresponding author address: Dr. Karen J. H. Thomas, School of Ocean Sciences, Marine Science Laboratories, University College of North Wales, Menai Bridge, Gwynedd, LL59 5EY, UK

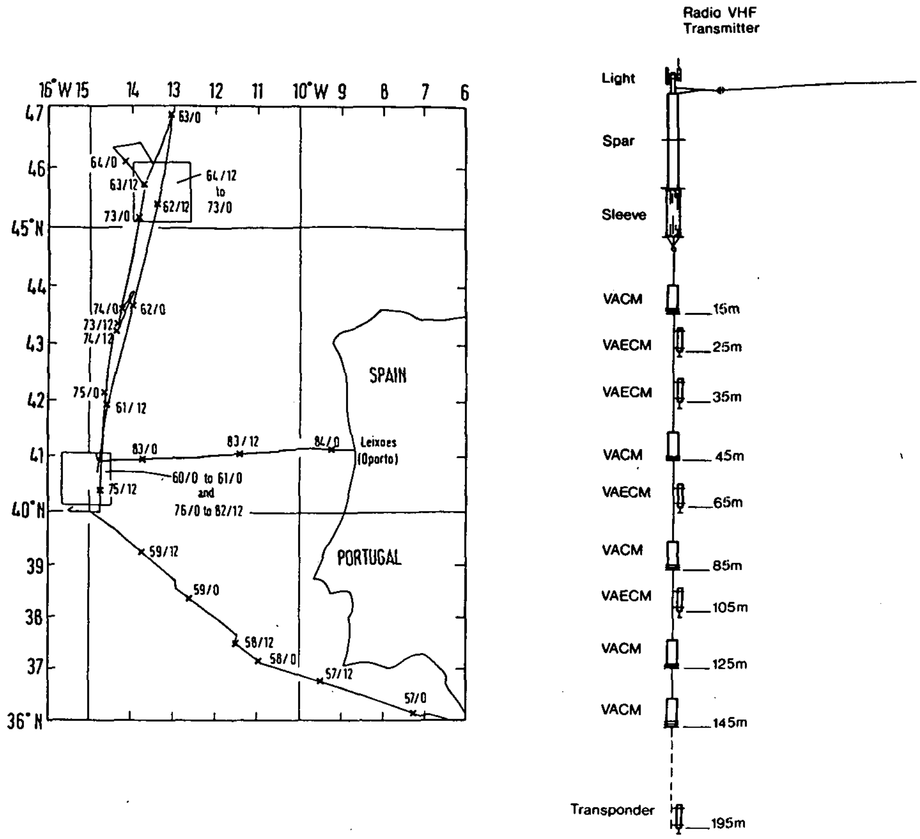

FIG. 1. (a) Ship's track plot, *RRS Discovery* Cruise 145. Day number in 1984 and time (UTC) along the track are annotated. (b) Drifting spar buoy rig as deployed, showing current meter depths. Data from the VACMs are discussed here.

discussing the model and results, we shall summarize briefly the important details of Langmuir circulations that determine the specification of the model.

2. Langmuir circulations

The observations and generation theories of Langmuir circulations have been reviewed by Pollard (1977) and Leibovich (1983). There are two mechanisms by which such longitudinal roll vortices may be generated in the ocean: instability of the Ekman layer (Faller 1971; Brown 1980) and wave–current interaction (Craik and Leibovich 1976; Craik 1977; Leibovich and Paolucci 1980).

Observations of Langmuir circulations have been reported sporadically since Langmuir's original measurements (Langmuir 1938). Row spacing (i.e. distance between convergence zones, or twice the cell width) has been found to vary between 2 and 25 m in lakes, and 2 and 300 m in the ocean. Some observations suggest that row spacing is related to the depth of the thermocline (Langmuir 1938; Scott et al. 1969). Assaf et al. (1971) studied Langmuir circulations off Bermuda in a deep water area (3000 m depth) and a shallow water area (50 m) on Plantagenet Bank. In the deeper water with a mixed layer depth (MLD) of 200 m, they found cells of three distinct scales, the largest having 280 m row spacing, and the smaller 40 and 5 m. No evidence of current stratification associated with the Ekman spiral was observed. However, on the same day, in the shallow water, they did find evidence of the Ekman spiral, shown by plumes of dye at different depths. This time, no medium or large scale cells were observed, only the 4–5 m ones. Assaf et al. suggest that in the deep water, the rolls are caused by Ekman instability hence the absence of the Ekman spiral. In the shallow water, the mechanism might be wave-dominated since the Ekman spiral coexisted with the rolls. These observations would suggest a cell width of approximately the MLD, say 200 m in our case, and that the Ekman instability should be the driving mechanism in deep water.

Recently, studies of large longitudinal rolls in the open ocean off California have been undertaken from the research platform *FLIP* (Weller et al. 1985; Weller and Price 1988). At a depth of 23 m, Weller et al. report large downwelling velocities (20 cm s^{-1}) in association with substantial downwind horizontal velocities [also O(20) cm s^{-1}]. This downwelling velocity is about twice as large as previous reports (Leibovich

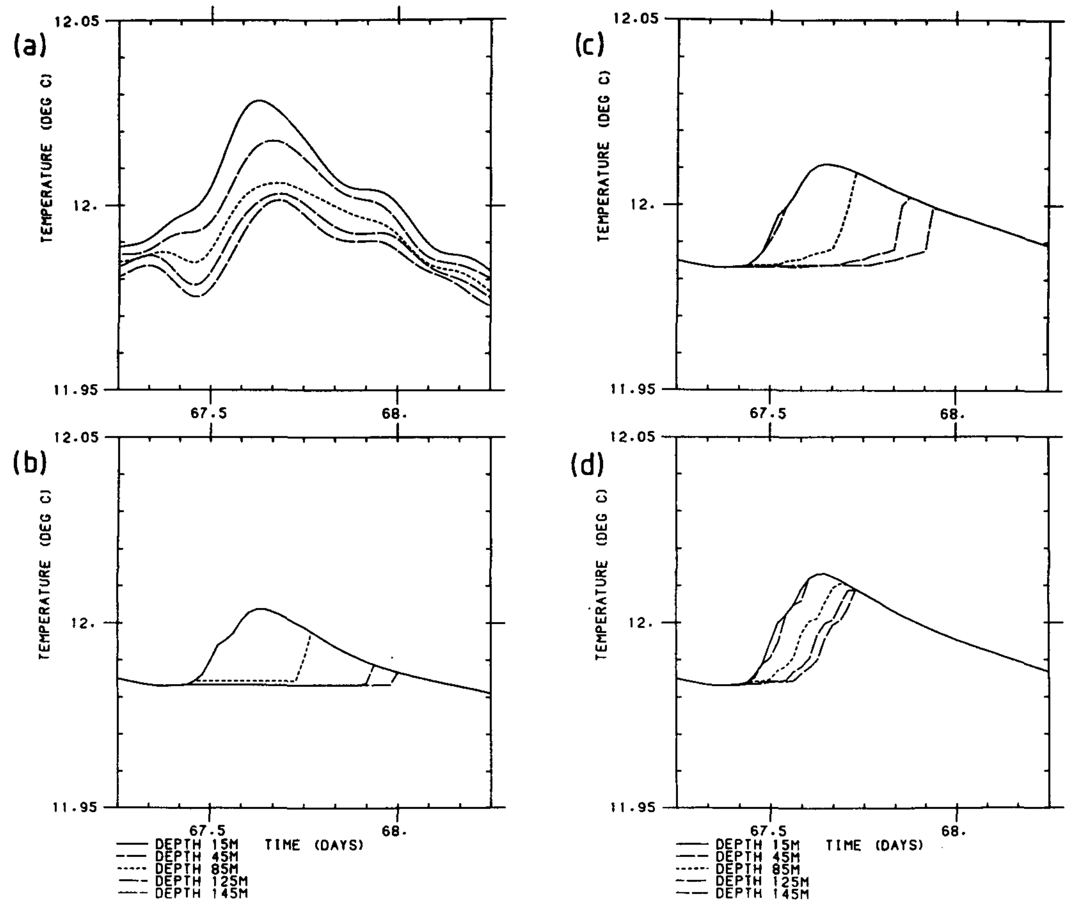

FIG. 2. (a) Observed temperature signal at the VACMs on 7 March 1984 (day number 67). Time is UTC. The data have been filtered to remove signals of less than 12 hours period. (b) Predicted temperature time series at the VACMs using the one-dimensional Kraus-Turner model. (c) Predicted temperature time series at the VACMs using the two-dimensional model imposing the advection field of Fig. 3. (d) As in (b) but with velocities four times greater.

1983) would suggest. However, the downwelling velocities were strongly depth dependent, being maximum between 10 and 35 m in the middle of the mixed layer. Downwelling velocities above and below were smaller, typically less than 5 cm s^{-1}. Weller and Price (1988) analyze the data further and present observations from MILDEX (the Mixed Layer Dynamics Experiment), confirming the picture of strong downwelling maxima in the middle of the mixed layer. A linear relation between downwelling speeds and wind speeds was not found. Cells on many scales were observed, the largest row spacing being revealed by Doppler sonar (Smith et al. 1987) to be three times the MLD. Again these observations suggest that a cell width of the same order of magnitude as the MLD would be applicable to our model. Leibovich and Lele (Leibovich 1985; Lele 1985) study the effects of imposing a mixed layer bounded by a thermocline on the development of cells due to wave–current interaction, and find that the rolls cannot penetrate below the thermocline provided that "the temperature gradient is sufficiently strong and the thermocline is sufficiently thick" (Leibovich 1983).

Small-scale Langmuir circulations are probably caused by the interaction of a surface wave field with a sheared current. Large-scale rolls might be caused either by a wave–current interaction or the inherent instability of the Ekman sheared layer. Many oceanographers (e.g. Leibovich 1983) use the term "Langmuir circulation" to describe only wave-generated rolls, since they believe that all the observed rows can be explained by a cascade of energy from small to large scale circulations. Some of the observations (e.g. Assaf et al. 1971) do however imply that the Ekman instability is a likely driving force and one cannot ignore this mechanism when considering large scale rolls, such as Langmuir's original observations.

The wave–current interaction theories predict a narrow downwelling zone with velocities greatest at the surface, whereas the Ekman instability theory predicts a more symmetrical cell, with maximum downwind velocities occurring not at the surface, but near half the cell depth. Both theories predict cell widths to be about the same size as cell depths (and therefore MLDs). It seems likely that in any given oceanic situation, both mechanisms will be at work, each to a greater or lesser degree. This is confirmed by the recent measurements of Weller et al. (1985) and Weller and Price (1988). The downwelling is much more energetic than the upwelling, indicating asymmetry in the cell. However, maximum downwind velocities are observed at half the depth of the cell in the downwelling regions, with small downwind velocities near the surface.

Langmuir circulations are not a fixed, steady-state structure. The evidence suggests a constantly changing flow, with cells growing until bounded by the thermocline, and smaller cells continually being formed. The rolls will interact with, and be advected by, the mean flow, and will always be altering due to changing wind or wave fields. Bearing this in mind, however, we can select likely scales for the Langmuir cell to be imposed in our model, based on the observations and modeling results discussed here. If the roll has grown to its largest extent, inhibited only by the thermocline (this is likely since the wind had been steady in speed and direction for several days prior to the spar deployment), then we would expect both cell width and cell depth to be similar in magnitude to the MLD. We shall therefore impose a cell of width and depth 200 m. Following the observations of Weller et al. (1985), we shall require that the circulation have narrow downwelling and broader upwelling zone, with maximum vertical velocities occurring at half the depth of the cell.

3. The model

The time series of temperatures at the current meters beneath the spar buoy might be modeled using a simple one-dimensional mixed layer model to predict $T(z, t)$. However, since there is an imbalance in the heat budget, a one-dimensional model would be inadequate. Therefore, in order to determine the nature of the Langmuir circulation required to simulate the observations, and to study its effect on mixed layer structure, a two-dimensional model has been developed. The model consists of a row of ten one-dimensional Kraus–Turner models (Kraus and Turner 1967) implemented on a grid of levels following Thompson (1976).

Each one-dimensional mixed layer model predicts temperature as a function of time at each of the levels, given the buoyancy flux and wind energy input at the surface; these processes will be described later. The models span the circulation in the x-direction, across the roll. The individual models are connected by an imposed velocity field, used to advect the temperature field both vertically (z-direction) and horizontally (x-direction). Each model acts independently when forced by the surface cooling, heating or wind. No mixing or diffusion of heat is imposed in the horizontal direction, and there is no mixing of momentum allowed.

The model assumes that the ocean is uniform in the along-roll (y) direction, since temperature variations are expected to be much smaller than in the across-roll direction. On the other hand, it is known that the along-roll velocity is much greater in the surface convergence zone than in the divergence region, but these along-roll velocities have been ignored for simplicity.

A further assumption is that the temperature of the water in a given column may become mixed by the wind and/or convection, but the velocity field is not allowed to be mixed. Observations (e.g. Scott et al. 1969) show that Langmuir circulations do exist in a well-mixed (in temperature) layer. It is envisaged that there are two different scales of mixed layer flow. The Langmuir cell is pictured as a large-scale (of order 200 m), slow (compared to turbulence) circulation, whereas the convection and wind mixing are assumed to be small scale, rapid, turbulent motions. We therefore consider only the heat budget of the model, not the momentum budget.

The imposed velocity field must be nondivergent; heat may only be advected in the plane perpendicular to the roll axis. It is also required that the velocity field be a smooth circulation with a narrow downwelling region and broad upwelling zone. A solution that neatly fits this requirement is that found by Stommel (1948) for wind-driven horizontal currents in a rectangular ocean (Fig. 3a). This also has a narrow, swiftly flowing region and a broad return flow (no analogy between the two phenomena is intended here; the Stommel solution, rotated from the horizontal plane to the vertical plane, is simply a suitable flow field which supplies most of the desired characteristics of the Langmuir cell). The flow is symmetrical in the vertical about the 100 m depth. The magnitude of the streamfunction itself is arbitrary here, since it is the gradient of the streamfunction that determines the velocity. Thorpe (1984) models the effect of Langmuir circulations on the distribution of submerged bubbles, and applies a similar two-dimensional velocity field. His streamfunction is however sinusoidal (and therefore symmetrical) in both x and z directions.

The model grid has a spacing of 5 m in the vertical and 20 m in the x-direction. The vertical resolution determines the precision of the mixed layer model; a large vertical grid spacing would smear out the heating signal and the exponential decrease of solar radiation with depth would not be resolved. Tests showed no significant differences between 5 and 1 m vertical resolution (Thomas 1987). The horizontal grid spacing is not as critical since the only process occurring horizontally is advection, so 20 m was chosen since it adequately defines the circulation required. The effects of reducing the horizontal grid spacing to decrease numerical diffusion will be discussed in the next section. Temperature T and streamfunction ψ are defined at the centres of each grid box, while velocities u and w are calculated at the corners. A mean velocity across each side of the grid box is calculated. The total depth of the model is 300 m but velocities are defined to be zero below 200 m, since we assume that velocities in

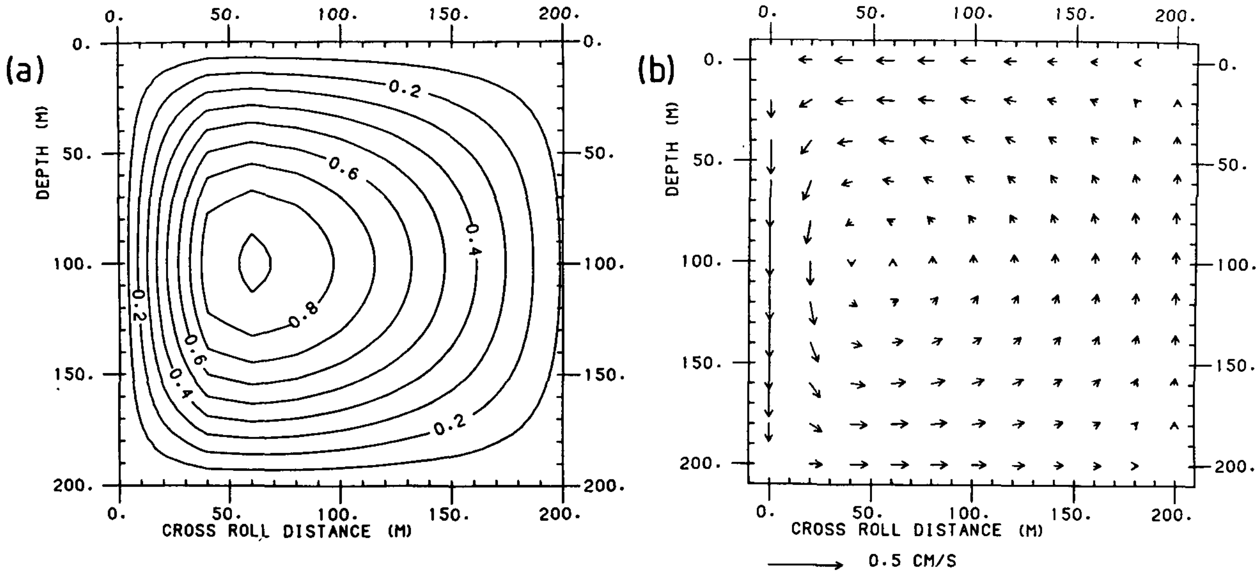

FIG. 3. (a) Streamlines of the nondivergent velocity field (Stommel solution) applied to the row of one-dimensional models. Grid spacing is 5 m in the vertical and 20 m in the horizontal direction. (b) Velocity field calculated from streamlines in (a). Velocities apply to the point at the tail of the arrow. Arrows are only drawn every 20 m in the vertical for clarity.

the thermocline are small compared to the rapid circulation in the Langmuir cell. Maximum vertical velocities are at half the depth of the cell, as Weller et al.'s (1985) observations of Langmuir circulations suggested. The edges of the cell are free-slip boundaries, thus velocities along the boundaries are larger than in the interior. The mean vertical velocity through the grid boxes of the far left-hand column is 0.175 cm s^{-1} while the maximum value is 0.275 cm s^{-1}. For comparison, the mean upwelling in the far right-hand column is 0.045 cm s^{-1}. Model runs with increased velocities will be discussed in section 5.

To summarize, the circulation model consists of ten mixed layer models, which determine the warming of each grid box at each time step. The grid boxes are connected by advection from box to box using an imposed velocity field. At each time step, the following procedure is carried out in the model:

1) Absorb surface heat fluxes (sensible and latent heat fluxes, longwave radiation) in each column. The absorption of solar radiation is described by a fit to observations of irradiance with depth (Thomas 1987). Other surface heat fluxes are absorbed in the uppermost layer.

2) Advect water both vertically and horizontally using the imposed velocity field (Fig. 3b). An upstream differencing scheme is used (Roache 1976).

3) Mix from the surface downwards using the procedure described by Thompson (1976, 1977a, 1977b), treating each column individually as a one-dimensional Kraus-Turner mixed layer model. The potential energy is taken as 1.25 times the wind energy, 15% penetrative convection is allowed, and an exponential decay of energy with depth is imposed (Elsberry et al. 1976) with a scale depth of 40 m. Briefly, each box is considered in turn, starting at the surface and working downwards. The potential energy required to mix the next level down into the mixed layer is compared to the energy available both from the wind and from potential energy released further up (due to dynamic instability). Mixing occurs if there is sufficient energy, and the available mixing energy is updated accordingly.

The Courant-Friedrichs-Lewy (CFL) condition (Roache 1976) provides a constraint on the maximum velocities allowed for a given time step and grid spacing. This requires that the vertical side of a grid box may not be smaller than the product of the time step and the vertical velocity into the box (and vice versa for the horizontal side of a box); in other words, water may not cross more than one box in each time step. The critical (i.e. largest) velocity is the vertical velocity at a depth of 100 m on the left-hand side. Later we shall see some runs where the magnitude of the whole flow field was increased by a factor of 4; under these conditions it was necessary to reduce the time step to avoid violating the CFL condition.

4. Test runs

We can show that the total heat content of the whole domain is conserved by applying zero surface fluxes and allowing heat to be advected within a cell (Figs. 4a and 4b). After 24 hours, warmer water is penetrating below cooler water from the left. In a real ocean this would create a static instability and overturning would occur. A standard numerical procedure has been added

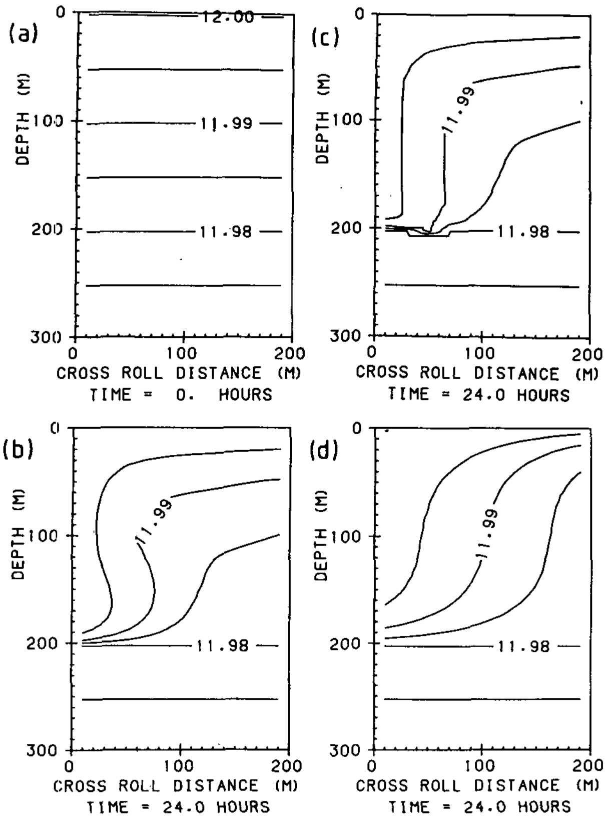

FIG. 4. Evolution of the temperature field across the cell; (a) is the initial state and (b) 24 hours later. Heat is advected according to the velocity field in Fig. 3. Temperature isotherms are plotted every 0.005°C. (c) As in (b) but allowing convective overturning where advection carries warmer water beneath cooler water. (d) As in (c) but imposing a symmetrical velocity field.

after stage 3 of the model to allow convective overturning under such circumstances. The profile is adjusted iteratively to create a layer of uniform temperature beneath the stratified region, eliminating static instability (Fig. 4c). The overturning entrains some of the water below 200 m into the mixed layer. Strictly, when this occurs, the velocity field should extend to the base of the mixed layer, since the Langmuir cell grows until it reaches the large density gradient of the thermocline (Leibovich 1983).

Test runs were also performed using a velocity field symmetrical across the roll as well as in the vertical (Fig. 4d); w varies with depth in the same way as it varies with x, i.e. sinusoidally. The speeds were scaled so that the strength of the circulation was approximately the same as the asymmetrical case. The downwelling zone is much less pronounced, and the heating effect takes nearly twice as long to reach the lower depths. A more significant effect is therefore obtained if the more realistic, asymmetrical cell is imposed.

Since an upstream differencing scheme is used for the advection, some numerical diffusion is implicit in the scheme. Tests were performed to see whether the effect of numerical diffusion would dominate the results obtained by the model (for details see Thomas 1987). The numerical diffusion is reduced if a smaller grid spacing is used (Roache 1976). To test whether a reduced numerical diffusion would significantly affect the model results, the model was run using a sinusoidal heating function and constant wind stress. Figure 5 shows the development of the temperature structure across the roll using the standard horizontal grid spacing of 20 m, while Fig. 6, for comparison, has less numerical diffusion since a grid spacing of 5 m was used. The reduction in numerical diffusion has had very little effect. For example, the 11.99°C isotherm has reached a depth of about 180 m at 1800 in both Figures; the 12.06°C isotherm is also in a very similar position. It is concluded that the numerical diffusion does not dominate the genuine processes in the model.

We shall now consider what physical processes are revealed in Fig. 5. After 6 hours a small thermocline has developed at about 50 m, the limit at which wind stirring and solar heating balance. This strengthens during the afternoon until there is considerable (approximately 0.005°C m^{-1}) stratification near 50 m at 1800. In the downwelling zone, however, the heat has

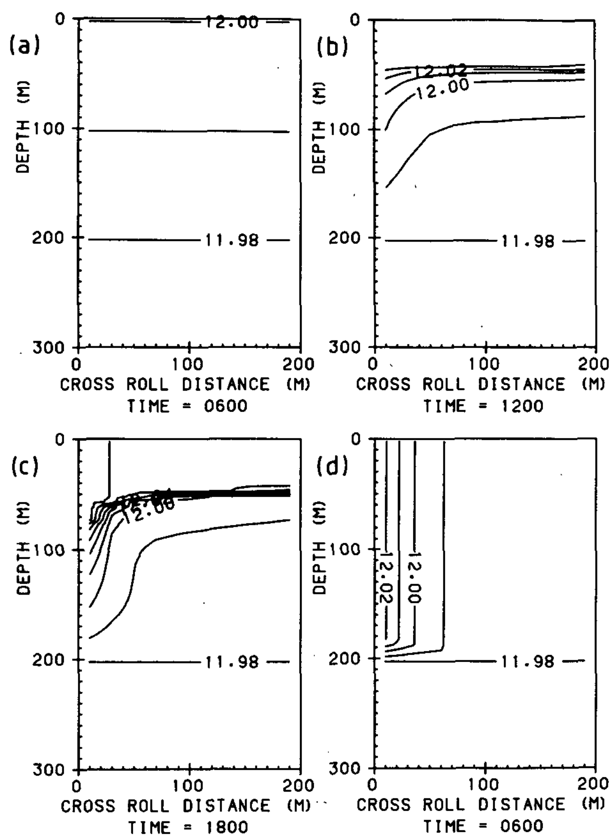

FIG. 5. Evolution of the temperature field at intervals of 6 hours with a sinusoidal heating function and constant wind stress. The initial state at 0600 is shown in the first graph. The contour interval is 0.01°C.

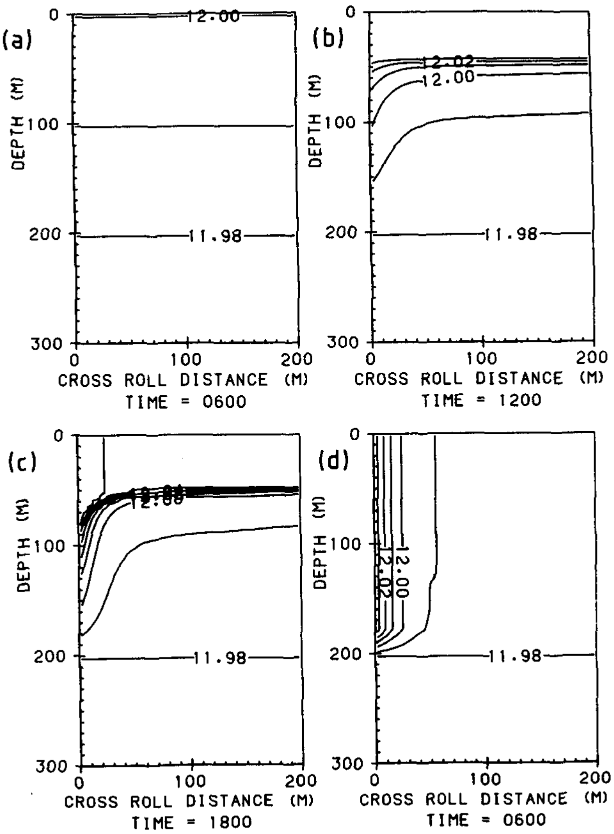

FIG. 6. As in Fig. 5 but using a horizontal grid spacing of 5 m so that less numerical diffusion is inherent in the advection scheme.

traveled much farther downwards, and there is stratification to 200 m. The final plot shows the temperature field at 0600 the following day, 24 hours after the start of the run. By this time a horizontal temperature gradient has become apparent, with warmer water on the left, in the downwelling zone.

It is interesting to examine the left-hand side of the model domain since this is where the spar buoy would be expected to drift. Temperature profiles at the left-hand side are shown in solid lines in Fig. 7a, while the dotted lines represent the model with no advection applied. The total heat content of the left-hand column at the end of the 24 hours is considerably larger in the advection model. Between the surface and 200 m, the mixed layer is on average 0.3°C warmer than in the one-dimensional model. The final MLD is nealy 100 m greater than without advection. The downward transport of the absorbed solar radiation may be followed from profile to profile as the stratified section of the curve progresses downwards below the mixed portion.

Obviously the advection is affecting the amount of heat transported into the ocean on the left-hand side. But is the circulation affecting the mean downward heat transport across the roll, or do the upwelling and downwelling balance out? Figure 7b (solid lines) shows average profiles using all ten columns across the roll. The circulation does indeed affect the mean downward heat transport of the whole region. The circulation has hastened the mean transport of heat into the ocean. After 24 hours, the water below about 100 m is some 5–10 mK warmer than it is without the circulation, whereas above 100 m it is cooler by a similar amount. This would imply that Langmuir circulations have a significant effect on the apparent eddy diffusion coefficient of heat. Thus, it is important to know whether Langmuir circulations are present during an experimental investigation of the mixed layer. Models that predict MLD or sea surface temperature may need to use a larger eddy diffusion coefficient if Langmuir circulations are (or are likely to be) present.

5. Simulation of the observations

Obviously the imposed circulation does help to carry heat downward faster and deeper than the one-dimensional model can achieve with wind mixing alone. It should help to simulate the temperature time series

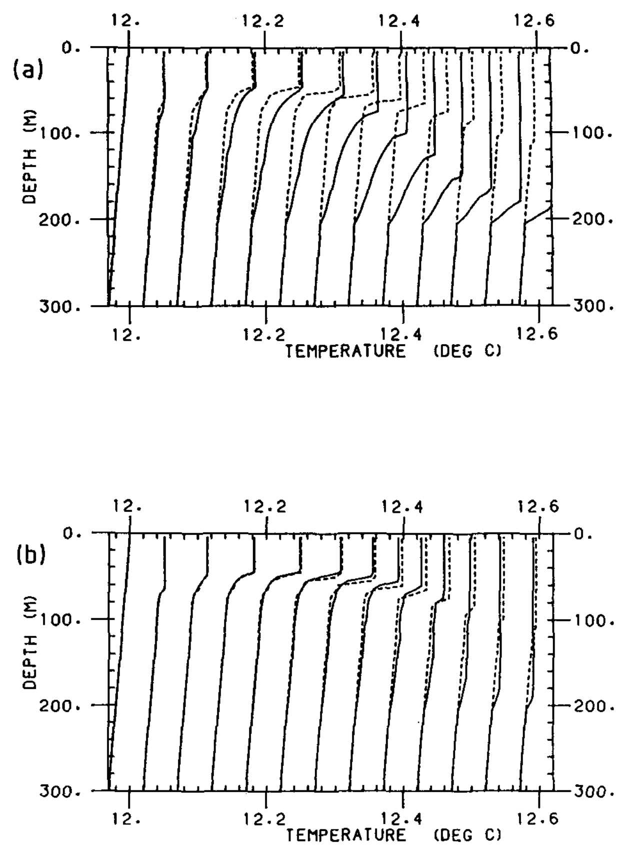

FIG. 7. (a) Temperature profiles on the left-hand side of the model circulation, plotted every 2 hours with an offset of 0.05°C. The results are with (solid lines) and without (dotted lines) the advection field of Fig. 3. (b) Average temperature profiles across the circulation with (solid lines) and without (dotted lines) advection. Otherwise as (a).

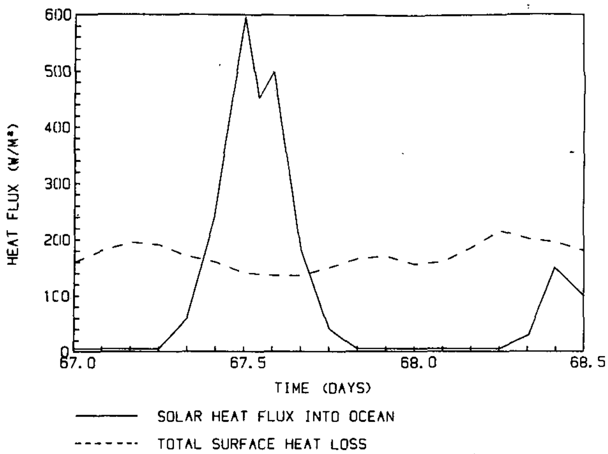

FIG. 8. Net downward shortwave heat flux and net surface heat loss during day 67 (7 March 1984).

observed at the VACMs, if we assume that the spar buoy drifts into the downwelling region of the roll. Therefore the model was run with real meteorological forcing and a more realistic initial condition, to investigate the magnitude of its effect in our case study.

In order to examine the heating signal in more detail, the first day only (day 67) will be considered (Fig. 2a). This was the sunniest day, and the anomaly in the heat budget was the largest (Fig. 8), so the required circulation will be strongest. The wind velocity was constant at approximately 13 m s^{-1} from the east. In Fig. 2b is shown the diurnal signal predicted by the Kraus-Turner model with no advection. Figure 2c shows the result of imposing the velocity field of Fig. 3b, assuming the temperature sensors to lie in the downwelling zone of the cell. It is seen that the advection has slightly improved the simulation; at 15 m, the diurnal heating signal is some 10 mK larger. At 125 and 145 m, there is now a visible diurnal signal of about 20 mK. Although this is closer to the observed signal than the one-dimensional results are, the heating is still not reaching the lower depths quickly enough. The temperature field associated with this modeled time series is shown in Fig. 9, where isotherms are plotted every six hours. The contour interval here is 0.005°C and only isotherms above 11.95°C are shown. At 1800 the 11.99°C isotherm is about 50 m deeper on the left-hand side than it is in the middle or right-hand side.

A series of runs was undertaken to investigate the effect of increasing the circulation strength on the amplitude and phase of the observed diurnal signal. For example, multiplying the velocity field of Fig. 3b by four increases the amplitude of the signal, and decreases the time lag between the signal reaching 15 m and the lower depths. For this velocity field, the mean downwelling in the left-hand grid boxes is 0.7 cm s^{-1}, while the maximum into any grid box is 1.1 cm s^{-1}. (In order to perform this run while satisfying the CFL condition, it was necessary to reduce the time step to 7.5 minutes instead of 0.5 hours). Figure 2d illustrates the modeled time series for this run.

The effect of increasing the imposed velocities is shown in Fig. 10. Circulation strength gives a measure of the speed of the circulation; the velocity field of Fig. 3 is defined to have a circulation strength of 1. The one-dimensional model has a circulation strength of 0; a circulation strength of 2 implies a velocity field twice as fast as that in Fig. 3. Figure 10a shows the time lag of the maximum of the diurnal signal between depths of 15 and 125 m. Error bars denote uncertainty in estimating the times of maximum diurnal signal. The time lag observed in the data lies somewhere between the two dotted lines. The required circulation strength is therefore approximately 4 to 6. Figure 10b illustrates the variation of the maximum amplitude of the diurnal signal at a depth of 45 m. The amplitude for a circulation strength of 8 is smaller than that for 4; this is because the advection is taking heat downwards more quickly; there is less stratification and the wind can mix more deeply.

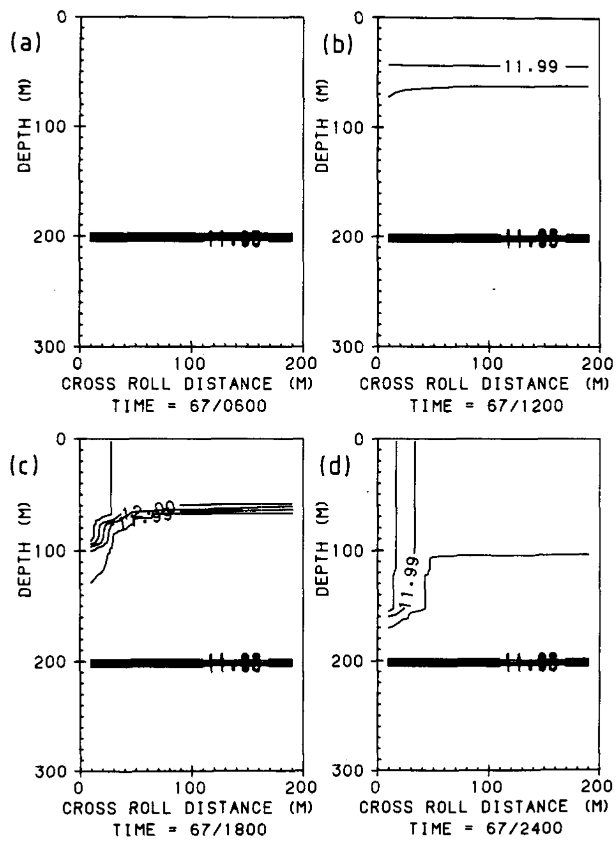

FIG. 9. Evolution of the temperature field across the roll during day 67. Isotherms greater than 11.95°C are plotted every 6 hours with a contour interval of 0.005°C. Advection is applied using the velocity field of Fig. 3.

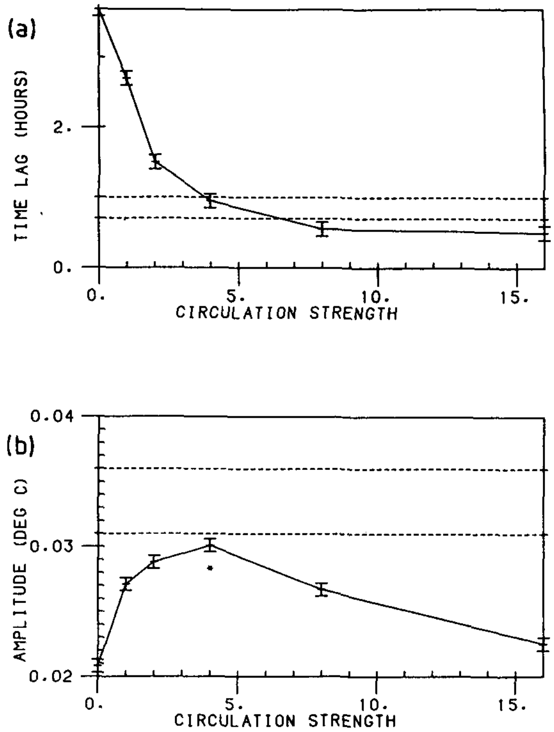

FIG. 10. Variation of the diurnal signal predicted by the model for various speeds of imposed circulation. (a) Time lag between depths of 15 and 125 m. (b) Amplitude at a depth of 45 m. The observed phase and amplitude lie between the dotted lines. The star shows the amplitude of the diurnal signal if a symmetrical circulation of strength 4 is imposed. The phase lag is the same as that obtained using an asymmetrical velocity field.

The observed amplitude of diurnal signal at 45 m lies somewhere between the two dotted lines. The circulation strength of 4 to 6 again seems the best fit to the data. However the modeled amplitude is still slightly smaller than that observed. The modeled signal could be increased by decreasing the width of the "boundary current" in the imposed velocity field. A narrower downwelling region would enhance the diurnal signal. To test this, the symmetrical velocity field was applied. Even though the maximum downwelling velocity is the same, the modeled diurnal signal is smaller in magnitude, because the warm water is not swept in as quickly at the surface. The star in Fig. 10b gives the amplitude of the signal if a symmetrical circulation of strength 4 is imposed; it is smaller than the asymmetric case. However the phase lag is indistinguishable from that using the asymmetrical circulation of the same strength.

6. Discussion

This model was not developed in order to simulate exactly the temperature time series at the VACMs. We recognize that it is an oversimplification of the processes determining upper-ocean structure. It was intended as a tool to see whether the assumption of a Langmuir circulation improved our understanding of the diurnal signal, and if so, what the likely magnitude of the circulation would be. It must be remembered that there are several approximations in the model that limit its realism. The assumption that the circulation may be modeled by a two-dimensional roll implies that the horizontal along-roll temperature variations are small compared to those across the roll.

The model assumes that the roll size is fixed at 200 m wide and 200 m deep. These dimensions were chosen after consideration of the SeaSoar data (temperature and salinity observations in the mixed layer and thermocline, discussed in Part I), remembering that a Langmuir cell width is usually approximately equal to the depth of the mixed layer. The initial state prescribed in the model has a mixed layer of depth 200 m. Experimental evidence of Langmuir circulations shows that rolls tend to increase in size until limited by the depth of the thermocline. During the six-day model run, the mixed layer deepens by about 40 m and so the advection field should deepen also. The justification for keeping a fixed velocity field during daytime stratification is that the density gradient built up during the day is really very small compared to that in the thermocline. Leibovich (1985) and Lele (1985) found that a thick thermocline of large gradient was required to inhibit growth of the cell.

The model does not allow any mixing to take place in the horizontal direction and it can produce significant horizontal temperature gradients (for example, 20 mK across 100 m in Fig. 7a). Interestingly, horizontal temperature gradients of this order of magnitude are observed in the SeaSoar data (Part I; Thomas 1987). This is therefore not a major failing of the model. Although numerical diffusion occurs in the model since an upstream differencing scheme is used, this has been shown not to have a significant effect on the model results.

This simple model has shown that it is possible to quantify the effect of Langmuir circulations on the development of the mixed layer. The assumption of a circulation of width and depth 200 m does improve the simulation of the temperature time series at the VACMs. Tests to fit the phase and amplitude of the diurnal signal on day 67 at the depths of the VACMs showed that a "circulation strength" of about 4 to 6 is required. The mean vertical velocity in the far left-hand column is therefore approximately 0.7 cm s^{-1}, while the maximum is approximately 1.1 cm s^{-1}. Although this is much larger than is usually assumed for vertical velocities in the upper ocean (meters per day, at most), it is of the same order as vertical velocities measured in Langmuir circulations, and is much smaller than the downwelling velocities observed by Weller and Price (1988).

Such circulations will affect the mixing of heat and momentum in the mixed layer. It is both observed (Myer 1971) and numerically predicted (Leibovich and Paolucci, 1980) that heat is advected downwards at the convergence zones. Weller et al. (1985) observed temperature anomalies of about 15 mK in downwelling zones. When the near-surface temperatures were warmer than the interior of the mixed layer (midday) then positive temperature anomalies were detected in downwelling regions. Similarly at night, negative temperature anomalies were observed in downwelling zones. As pointed out by Faller (1971), the effective eddy viscosity is greatly increased by rolls.

Langmuir circulations will also affect the drifting of buoys. A possible example of this is documented by McNally and White (1985), who observe freely drifting buoys, drogued at various depths, having a large downwind velocity when they are in the mixed layer. The crosswind velocity component can be accounted for by considering a simple Ekman slab model (Davis et al. 1981) but the downwind velocity is larger than the windage, calculated from wind stress and drag coefficient, can predict. The buoys move in a direction about 30° to the right of the wind. By correlating the downwind velocity with the wind stress, it is found that the downwind current is wind-driven but lags the wind by 6 to 12 hours. McNally and White comment that "the large downwind residual velocity remains as yet unexplained". It is possible that neighboring storms created downwind currents (Price 1983). These observations might however imply that the buoys drifted into the convergence zone of a Langmuir circulation, since this would produce an anomalously large downwind velocity only while the buoy was in the mixed layer. It is known (Saunders, personal communication) that drifting buoys during JASIN exhibited a similar unexplained." It is possible that neighboring storms created unlikely that a longitudinal roll structure would exist in the upper ocean for several months, but one must remember that the drifting buoys might well drift from one convergence zone to another as the rolls evolve, grow, merge or die away. The possible presence of such circulations should therefore be borne in mind during any such drifting buoy experiment.

7. Conclusions

To our knowledge, this is the first attempt to combine the effects of Langmuir circulations with a mixed layer model. There is growing evidence (Weller and Price 1987; Pollard and Thomas 1988) that strong Langmuir circulations are commonly found in the open ocean even though they may not be obvious without weed or debris to delineate them. This model has shown that the presence of such rolls can help to mix heat into the upper ocean, and may also help to deepen the mixed layer. Heat is preferentially carried downwards at the convergence zones, where a freely-drifting instrument will experience an enhanced diurnal cycle of heating and cooling, as well as a larger downwind velocity than a simple slab model would predict.

Acknowledgments. This work was supported by a NERO CASE studentship award (GT4/83/AAPS/44) at the University of Southampton and the Institute of Oceanographic Sciences, Wormley. I would like to thank Steven Alderson for his help and advice in designing and running the model, and Neil Wells, Kelvin Richards and Peter Killworth for useful discussions. I am grateful to an anonymous referee for his constructive comments on the text.

REFERENCES

Assaf, G., R. Gerard and A. L. Gordon, 1971: Some mechanisms of oceanic mixing revealed in aerial photographs. *J. Geophys. Res.*, **76**, 6550–6572.

Brown, R. A., 1980: Longitudinal instabilities and secondary flows in the planetary boundary layer: A review. *Rev. Geophys. Space Phys.*, **18**, 683–697.

Craik, A. D. D., 1977: The generation of Langmuir circulations by an instability mechanism. *J. Fluid Mech.*, **81**, 209–223.

——, and S. Leibovich, 1976: A rational model for Langmuir circulations. *J. Fluid Mech.*, **73**, 401–426.

Davis, R. E., R. de Szoeke and P. Niiler, 1981: Variability in the upper ocean during MILE. *Deep-Sea Res.*, **28**(12A), 1427–1475.

Elsberry, R. L., T. S. Fraim and R. N. Trapnell, 1976: A mixed layer model of the oceanic thermal response to hurricanes. *J. Geophys. Res.*, **81**, 1153–1162.

Faller, A. J., 1971: Oceanic turbulence and the Langmuir circulations. *Ann. Rev. Ecology Systematics*, R. F. Johnston et al., Ed., **2**, 201–236.

Kraus, E. B., and J. S. Turner, 1967: A one-dimensional model of the seasonal thermocline. II: The general theory and its consequences. *Tellus*, **19**, 98–106.

Langmuir, I., 1938: Surface motion of water induced by wind. *Science*, **87**, 119–123.

Leibovich, S., 1983: The form and dynamics of Langmuir circulations. *Ann. Rev. Fluid Mech.*, **15**, 391–427.

——, 1985: Dynamics of Langmuir circulations in a stratified ocean. *The Ocean Surface*, T. Toba and H. Mitsuyasu, Eds., Reidel, 457–464.

——, and S. Paolucci, 1980: The Langmuir circulation instability as a mixing mechanism in the upper ocean. *J. Phys. Oceanogr.*, **10**, 186–207.

Lele, S. K., 1985: Some problems in hydrodynamic stability arising in geophysical fluid dynamics. PhD dissertation, Cornell University.

McNally, G. J., and W. B. White, 1985: Wind-driven flow in the mixed layer observed by drifting buoys during autumn–winter in the midlatitude North Pacific. *J. Phys. Oceanogr.*, **15**, 684–694.

Myer, G. E., 1971: Structure and mechanics of Langmuir circulations on a small inland lake. PhD dissertation, State University of New York, Albany.

Pollard, R. T., 1977: Observations and theories of Langmuir circulations and their role in near surface mixing. *A Voyage of Dis-*

covery: George Deacon 70th Anniversary Volume, M. Angel, Ed., Pergamon, 235–251.

——, and K. J. H. Thomas, 1989: Vertical circulation revealed by diurnal heating of the upper ocean in late winter. Part I: Observations. *J. Phys. Oceanogr.*, **19**, 269–278.

Price, J. F., 1983: Internal wave wake of a moving storm. Part I: Energy budget and observations. *J. Phys. Oceanogr.*, **13**, 949–965.

Roache, P. J., 1976: *Computational Fluid Dynamics*. Revised printing, Hermosa Publishers, 446 pp.

Scott, J. T., G. E. Myer, R. Stewart and E. G. Walther, 1969: On the mechanism of Langmuir circulations and their role in epilimnion mixing. *Limnol. Oceanogr.*, **14**, 493–503.

Smith, J., R. Pinkel and R. Weller, 1987: Velocity structure in the mixed layer during MILDEX. *J. Phys. Oceanogr.*, **17**, 425–439.

Stommel, H., 1948: The westward intensification of wind-driven ocean currents. *Trans. Amer. Geophys. Union*, **99**, 202–206.

Thomas, K. J. H., 1987: A Lagrangian study of the diurnal heating of the upper ocean. PhD thesis, University of Southampton.

Thompson, R. O. R. Y., 1976: Climatological numerical models of the surface mixed layer of the ocean. *J. Phys. Oceanogr.*, **6**, 496–503.

——, 1977a: Erratum on 'Climatological numerical models of the surface mixed layer of the ocean. *J. Phys. Oceanogr.*, **7**, 157.

——, 1977b: Reply. *J. Phys. Oceanogr.*, **7**, 470–471.

Thorpe, S. A., 1984: The effect of Langmuir circulation on the distribution of submerged bubbles, caused by breaking wind waves. *J. Fluid Mech.*, **142**, 151–170.

Weller, R. A., and J. F. Price, 1988: Langmuir circulation within the oceanic mixed layers. *Deep-Sea Res.*, **35A**(5), 711–747.

——, J. P. Dean, J. Marra, J. F. Price, E. A. Francis and D. O. Boardman, 1985: Three-dimensional flow in the upper ocean. *Science*, **227**, 1552–1556.